Catalysis Today 156 (2010) 254–260

Contents lists available at ScienceDirect

Catalysis Today

journal homepage: www.elsevier.com/locate/cattod

Methanol steam reforming in a dual-bed membrane reactor for producing PEMFC grade hydrogen

Sandra Sá [a], José M. Sousa [a,b], Adélio Mendes [a,*]

[a] LEPAE-Departamento de Engenharia Química, Faculdade de Engenharia da Universidade do Porto, Rua Dr. Roberto Frias, 4200-465 Porto, Portugal
[b] Departamento de Química, Universidade de Trás-os-Montes e Alto Douro, Apartado 202, 5001-911 Vila-Real Codex, Portugal

ARTICLE INFO

Article history:
Available online 15 March 2010

Keywords:
Hydrogen
Methanol steam reforming
PROX reaction
Carbon molecular sieve membranes
Modelling

ABSTRACT

This work focus on the advantages of adding a preferential carbon monoxide oxidation (PROX) reactor to a common methanol steam reforming (SR) membrane reactor (MR). The study was performed by using a one-dimensional mathematical model, assuming axially dispersed plug flow with pressure drop in both retentate and permeate sides. The finite volumes method was used for space discretization, being the dependent variables determined using high-resolution schemes.

The simulation results showed clear advantages of the SR + PROX towards the SR membrane reactor in what concerns the amount of CO in the permeate stream. More specifically, the permeate CO concentration in the SR + PROX MR was reduced to levels below 2 ppm, enabling the stream to feed a fuel cell. Additionally, high values of methanol conversion and hydrogen recovery were achieved, and the amount of CO_2 at the permeate side was able to remain below 20% for all simulations.

1. Introduction

Polymer electrolyte membrane fuel cells (PEMFC) are a promising source of clean electrical power for small scale and transport applications [1–4]. However, these devices require hydrogen as fuel, which presents storage and transportation problems. The need to overcome these problems makes *in situ* hydrogen production from alcohols and hydrocarbons steam reforming very attractive [5–7]. In comparison to other fuels, methanol presents several advantages which justify its application as a hydrogen carrier for fuel cell applications. More specifically, methanol is liquid at atmospheric conditions, has high hydrogen to carbon ratio, and its reforming temperature is relatively low (200–300 °C) [8–10].

According to the literature [11,12], there are three chemical reactions to be considered in a methanol steam reformer: the methanol steam reforming (SR, Eq. (1)), which is the main reaction, and the methanol decomposition (MD, Eq. (2)) and water gas shift (WGS, Eq. (3)) side reactions:

$$CH_3OH + H_2O \rightleftharpoons CO_2 + 3H_2 \quad \Delta H = 49.7\ \text{kJ mol}^{-1} \tag{1}$$

$$CH_3OH \rightleftharpoons CO + 2H_2 \quad \Delta H = 92.0\ \text{kJ mol}^{-1} \tag{2}$$

$$CO + H_2O \rightleftharpoons CO_2 + H_2 \quad \Delta H = -41.2\ \text{kJ mol}^{-1} \tag{3}$$

The major disadvantage of this process is the formation of carbon monoxide as a secondary product. It is known that carbon monoxide poisons the anodic catalyst of the fuel cell, so it must be reduced to levels under than 10 ppm [13]. In the same way, carbon dioxide can also have negative effect on the performance of the fuel cell, and its concentration should be maintained below 20% [14]. The latter effect is probably due to the formation of carbon monoxide by the reverse water gas shift reaction.

The separation of hydrogen from the resulting gas mixture can be accomplished by using a permselective membrane. The use of palladium (Pd) membranes for hydrogen separation in membrane reactors is very common and is vastly reported in the literature [9,15–20], due to their high selectivity to hydrogen. However, these membranes are expensive and have limited applications due to their low permeability compared to porous inorganic membranes [21,22]. Another type of membranes that can be used to perform such separation are the carbon molecular sieve (CMS) membranes. These membranes are less expensive and present higher permeabilities than Pd membranes, enabling the use of higher feed flow rates. However, they are brittle and permeable to other species besides hydrogen. Regarding the application of these membranes, Zhang et al. [10] compared a traditional reactor with a CMS membrane reactor for the methanol steam reforming reaction, concluding that higher conversion and lower carbon monoxide yield could be achieved. Harale et al. [23] studied a CMS membrane reactor for the water gas shift reaction and presented membranes with very high hydrogen permeation fluxes. These studies showed that higher flow rates and lower membrane areas can be used with

* Corresponding author. Tel.: +351 22 508 1695; fax: +351 22 508 1449.
E-mail address: mendes@fe.up.pt (A. Mendes).

0920-5861/$ – see front matter © 2010 Elsevier B.V. All rights reserved.
doi:10.1016/j.cattod.2010.02.030

Nomenclature

A	area, m^2
C^T_{S1}	total catalyst surface concentration of site 1, mol m^{-2}
C^T_{S1a}	total catalyst surface concentration of site 1a, mol m^{-2}
Da	Damköhler number
D_{ax}	axial dispersion coefficient, $m^2\ s^{-1}$
d_p	catalyst diameter, m
F_i	dimensionless molar flow rate of species i
k_i	rate constant for reaction i, $m^2\ s^{-1}\ mol^{-1}$
K^e_j	equilibrium constant for reaction j
K_i	adsorption coefficient for surface species i
$k_{PROX,ref}$	rate constant for the PROX reaction at the reference temperature, $m^2\ s^{-1}\ mol^{-1}$
$k_{SR,ref}$	rate constant for the SR reaction at the reference temperature, $m^2\ s^{-1}\ mol^{-1}$
ℓ	reactor's length, m
L_i	permeance coefficient of species i, kmol $m^{-2}\ s^{-1}\ kPa^{-n}$
m_{cat}	mass of catalyst, kg
M_{ref}	reference molar mass, kg mol^{-1}
N_i	flux of the component i through the membrane, mol $s^{-1}\ m^{-2}$
Pe	*Peclet* number for mass transfer
p_i	partial pressure of component i, kPa
P_{ref}	reference pressure, kPa
P	total pressure, kPa
$\Re$	gas constant, kPa $m^3\ mol^{-1}\ K^{-1}$
r_j	rate of reaction j, mol $s^{-1}\ m^{-2}$
r^R	radius of the reactor, m
R_i	rate of consumption or formation of species i, mol s^{-1} kg cat^{-1}
R_A	ratio between the retentate and permeate areas
$R_{m_{cat}}$	ratio between the permeate and retentate catalyst mass
S_A	surface area of the catalyst, $m^2\ kg^{-1}$
T	absolute temperature, K
u	Interstitial velocity, m s^{-1}
u_{ref}	reference velocity, m s^{-1}
x	relative length of the reactor
z	length of the reactor, m
ε	void fraction of the catalyst bed
Γ	contact time
μ	gas viscosity, kg $m^{-1}\ s^{-1}$
θ	dimensionless time variable
ρ	gas density, kg m^{-3}
ρ_{cat}	catalyst density, kg cat m^{-3}
υ_{ij}	stoichiometric coefficient for species i in the reaction j

Superscripts

M	membrane
R	retentate
P	permeate

Subscripts

MD	methanol decomposition
PROX	preferential oxidation
RWGS	reverse water gas shift
SR	steam reforming
WGS	water gas shift

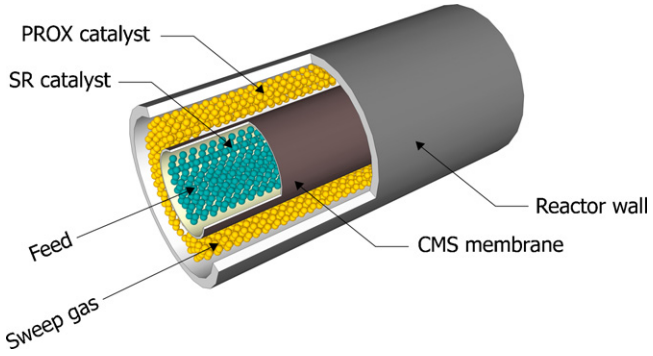

Fig. 1. Scheme of the simulated membrane reactor.

CMS membrane reactors. The major drawback of these membranes is the low selectivity towards hydrogen. Due to the CMS permeability to other species, the carbon monoxide concentration at the permeate side can exceed the imposed limit of 10 ppm. To reduce the amount of carbon monoxide, several approaches can be made, namely the preferential oxidation and the water gas shift reactions. Comparing both reactions, the WGS has the advantage of producing hydrogen while consuming carbon monoxide. However, due to thermodynamic limitations, the reaction conversion does not achieve 100% and the final carbon monoxide concentration exceeds 10 ppm [24]. On the other hand, the PROX reaction can easily convert the majority of the carbon monoxide that permeates through the membrane, but some hydrogen is consumed in the process. Due to the importance of the carbon monoxide removal of the permeate stream, the PROX reaction will be used in this work. According to the literature [25], the CO oxidation (Eq. (4)) and the H_2 oxidation (Eq. (5)) reactions must be considered:

$$CO + 1/2O_2 \rightarrow CO_2 \quad \Delta H = -283\ kJ\,mol^{-1} \tag{4}$$

$$H_2 + 1/2O_2 \rightarrow H_2O \quad \Delta H = -242\ kJ\,mol^{-1} \tag{5}$$

This work simulates the production of hydrogen by methanol steam reforming in a carbon molecular sieve membrane reactor. Low CO concentration is assured by a catalyst bed for the PROX reaction at the permeate side. The present work aims to compare the membrane reactor performance with and without the PROX reaction. Ultimately, the objective is to achieve a hydrogen rich permeate stream with low CO and CO_2 concentrations. To this end, a one-dimensional comprehensive mathematical model of a dual packed-bed membrane reactor was developed. The simulation results can help to find the best conditions for the membrane reactor operation. The main goals of this study are the achievement of the highest methanol conversion and hydrogen recovery, keeping the CO concentration at the permeate side below 10 ppm and the one of CO_2 below 20%.

2. Development of the membrane reactor model

Fig. 1 shows the scheme of the simulated membrane reactor. It consists in a tubular membrane with surface area A^M, housing a packed-bed of a SR catalyst in the retentate chamber and a packed-bed of a PROX catalyst in the permeate chamber. A gas phase stream of methanol and water is fed to the retentate side, producing hydrogen, carbon dioxide and carbon monoxide. Water vapour is used as sweep gas in the permeate side, flowing in co-current. Oxygen is also fed to the permeate chamber to perform the PROX reaction.

The mathematical model proposed comprises the steady-state mass balance equations for the reaction and permeation sides, as well as the respective boundary conditions.

This model is based on the following general assumptions: isothermal conditions, ideal gas behaviour, axially dispersed plug flow with pressure drop described by the *Ergun* equation [26], negligible radial gradients and uniform cross-sectional void fraction.

2.1. Retentate side

Partial mass balance

$$-\frac{d}{dz}\left(u^R p_i^R\right)+D_{ax}\frac{d}{dz}\left(P^R\frac{d}{dz}\left(\frac{p_i^R}{P^R}\right)\right)-\frac{2\pi r^M}{\varepsilon A^R}\Re T N_i+\frac{m_{cat}^R}{\varepsilon V^R}\Re T R_i^R=0 \tag{6}$$

Total mass balance

$$-\frac{d}{dz}(u^R P^R)-\frac{2\pi r^M}{\varepsilon A^R}\Re T\sum_i N_i+\frac{m_{cat}^R}{\varepsilon V^R}\Re T\sum_i R_i^R=0 \tag{7}$$

Pressure drop

$$-\frac{dP^R}{dz}=150\frac{\mu u^R}{d_p^2}(1-\varepsilon)^2+\frac{7}{4}\frac{\rho_{gas}(u^R)^2}{d_p}\frac{1-\varepsilon}{\varepsilon} \tag{8}$$

Boundary conditions

The partial mass balance is a second order differential equation, thus two boundary conditions are needed [27]. When the pressure drop cannot be considered negligible, it must be imposed one boundary condition in $z=0$ and other in $z=1$, as follows:

$$z=0:\ \varepsilon D_{ax}\frac{d}{dz}\left(\frac{p_i^R}{P^R}\right)=u^R\frac{p_i^R-p_i^{R,in}}{P^R}\quad\text{and}\quad u^R=u^{R,in} \tag{9}$$

$$z=1:\ \frac{d}{dz}\left(\frac{p_i^R}{P^R}\right)=0\quad\text{and}\quad P^R=P^{R,out} \tag{10}$$

where the superscript R stands for retentate side, i refers to the ith component, z is axial coordinate, u is the interstitial velocity, p is the partial pressure, P is the total pressure, D_{ax} is the effective axial dispersion coefficient, r^M is the internal radius of the membrane, A^R is the cross-sectional area of the retentate chamber, V^R is the volume of the retentate chamber, ε is the void fraction of the catalyst bed, $\Re$ is the gas constant, T is the absolute temperature, N is the flux through the membrane, and m_{cat} is the mass of catalyst, d_P is the catalyst particle diameter, μ is the gas viscosity and ρ_{gas} is the gas density. R is the rate of consumption or formation of the individual species, which is given by:

$$R_i=\sum_j \upsilon_{ij} r_j \tag{11}$$

where r_j is the reaction rate of reaction j (described below) and υ_{ij} is the stoichiometric coefficient for species i in the reaction j, taken negative for reactants, positive for reaction products, and null for the components that do not take part in the reaction.

Kinetic model – SR reaction

The reaction rate expressions used in this model are the ones developed by Peppley et al. [12]. It is assumed that the reaction occurs only at the catalyst surface, and that there is no mass transfer resistance between the bulk gas and the catalyst surface.

$$r_{SR}=\frac{k_{SR}K^*_{CH_3OH^{(1)}}\left(p_{CH_3OH}/p_{H_2}^{1/2}\right)\left(1-(p_{H_2}^3 p_{CO_2}/K^e_{SR}p_{CH_3OH}p_{H_2O})\right)C_{S1}^T C_{S1a}^T S_A}{\left(1+K^*_{CH_3OH^{(1)}}(p_{CH_3OH}/p_{H_2}^{1/2})+K^*_{HCOO^{(1)}}p_{CO_2}p_{H_2}^{1/2}+K^*_{OH^{(1)}}(p_{H_2O}/p_{H_2}^{1/2})\right)\left(1+K^{1/2}_{H^{(1a)}}p_{H_2}^{1/2}\right)} \tag{12}$$

$$r_{WGS}=\frac{k_{WGS}K^*_{OH^{(1)}}\left(p_{CO}p_{H_2O}/p_{H_2}^{1/2}\right)\left(1-(p_{H_2}p_{CO_2}/K^e_{WGS}p_{CO}p_{H_2O})\right)C_{S1}^{T2}S_A}{\left(\left(1+K^*_{CH_3OH^{(1)}}(p_{CH_3OH}/p_{H_2}^{1/2})+K^*_{HCOO^{(1)}}p_{CO_2}p_{H_2}^{1/2}+K^*_{OH^{(1)}}(p_{H_2O}/p_{H_2}^{1/2})\right)\left(1+K^{1/2}_{H^{(1a)}}p_{H_2}^{1/2}\right)\right)^2} \tag{13}$$

$$r_{MD}=\frac{k_{MD}K^*_{CH_3OH^{(2)}}\left(p_{CH_3OH}/p_{H_2}^{1/2}\right)\left(1-(p_{H_2}^2 p_{CO}/K^e_{MD}p_{CH_3OH})\right)C_{S2}^T C_{S2a}^T S_A}{\left(1+K^*_{CH_3OH^{(2)}}(p_{CH_3OH}/p_{H_2}^{1/2})+K^*_{OH^{(2)}}(p_{H_2O}/p_{H_2}^{1/2})\right)\left(1+K^{1/2}_{H^{(2a)}}p_{H_2}^{1/2}\right)} \tag{14}$$

where k_j and K_j^e are the reaction rate and equilibrium constants for reaction j, respectively; K_i is the adsorption coefficient for surface species i, C_{S1}^T and C_{S2}^T are the total catalyst surface concentration of sites 1 and 2, respectively, C_{S1a}^T and C_{S2a}^T are the total catalyst surface concentration of sites 1a and 2a, respectively, and S_A is the surface area of the catalyst.

2.2. Permeate side

Partial mass balance

$$-\frac{d}{dz}\left(u^P p_i^P\right)+D_{ax}\frac{d}{dz}\left(P^P\frac{d}{dz}\left(\frac{p_i^P}{P^P}\right)\right)+\frac{2\pi r^M}{\varepsilon A^P}\Re T N_i+\frac{m_{cat}^P}{\varepsilon V^P}\Re T R_i^P=0 \tag{15}$$

Total mass balance

$$-\frac{d}{dz}\left(u^P P^P\right)+\frac{2\pi r^M}{\varepsilon A^P}\Re T\sum_i N_i+\frac{m_{cat}^P}{\varepsilon V^P}\Re T\sum_i R_i^P=0 \tag{16}$$

Pressure drop

$$-\frac{dP^P}{dz}=150\frac{\mu u^P}{d_p^2}(1-\varepsilon)^2+\frac{7}{4}\frac{\rho_{gas}(u^P)^2}{d_p}\frac{1-\varepsilon}{\varepsilon} \tag{17}$$

Boundary conditions

$$z=0:\ \varepsilon D_{ax}\frac{d}{dz}\left(\frac{p_i^P}{P^P}\right)=u^P\frac{p_i^P-p_i^{P,in}}{P^P}\quad\text{and}\quad u^P=u^{P,in} \tag{18}$$

$$z=1:\ \frac{d}{dz}\left(\frac{p_i^P}{P^P}\right)=0\quad\text{and}\quad P^P=P^{P,out} \tag{19}$$

where superscript P stands for permeate side and A^P is the cross-sectional area of the permeate chamber.

Kinetic model – PROX reaction

The reaction rate expressions used in this model are the ones developed by Lee and Kim [28]:

$$r_{CO}=k_{CO}p_{CO}^{0.91}p_{CO_2}^{-0.37}p_{H_2O}^{-0.62} \tag{20}$$

$$r_{H_2}=k_{H_2}p_{H_2}p_{CO_2}^{-0.48}p_{H_2O}^{-0.69} \tag{21}$$

2.3. Membrane permeation equation

The mass transfer of each component through the membrane is assumed to be described by its local driving force and a global mass transfer coefficient, according to the following equation:

$$N_i(z)=L_i\left\{\left(p_i^R(z)\right)^n-\left(p_i^P(z)\right)^n\right\} \tag{22}$$

where L is a permeance coefficient and n is equal to 1 (CMS membrane). The film transport resistance supposed at the interface gas/membrane is considered negligible and the permeability coefficients are assumed constant.

2.4. Dimensionless equations

The model variables were made dimensionless with respect to the retentate feed velocity ($u^{R,in}$), to hydrogen (L_{H_2} and M_{H_2}) and to the reactor length, ℓ. Changing for dimensionless variables and introducing suitable dimensionless parameters, Eqs. (6)–(10), (15)–(19) and (22) become as follows:

$$-\frac{d}{dx}\left(u^{R*}p_i^{R*}\right)+\frac{1}{Pe}\frac{d}{dx}\left(P^{R*}\frac{d}{dx}\left(\frac{p_i^{R*}}{P^{R*}}\right)\right)-\Gamma T^* N_i^*+DaT^* R_i^{R*}=0 \quad (23)$$

$$-\frac{d}{dx}\left(u^{R*}P^{R*}\right)-\Gamma T^*\sum_i N_i^*+DaT^*\sum_i R_i^{R*}=0 \quad (24)$$

$$-\frac{dP^{R*}}{dx}=\alpha\mu u^{R*}+\beta\frac{\rho_{gas}^*}{T^*}|u^{R*}|u^{R*} \quad (25)$$

$$x=0:\ \frac{1}{Pe}\frac{d}{dx}\left(\frac{p_i^{R*}}{P^{R*}}\right)=u_{x=0}^{R*}\frac{p_i^{R*}-p_{i,x=0^-}^{R*}}{P^{R*}}\ \text{and}\ u^{R*}=u^{R,in*} \quad (26)$$

$$x=1:\ \frac{d}{dx}\left(\frac{p_i^{R*}}{P^{R*}}\right)=0\quad\text{and}\quad P^{R*}=P^{R,out*} \quad (27)$$

$$-\frac{d}{dx}\left(u^{P*}p_i^{P*}\right)+\frac{1}{Pe}\frac{d}{dx}\left(P^{P*}\frac{d}{dx}\left(\frac{p_i^{P*}}{P^{P*}}\right)\right)+\Gamma\Re_A T^* N_i^* +DaR_A R_{m_{cat}} R_\kappa T^* R_i^{P*}=0 \quad (28)$$

$$-\frac{d}{dx}\left(u^{P*}P^{P*}\right)-\Gamma\Re_A T^*\sum_i N_i^*+DaR_A R_{m_{cat}} R_\kappa T^*\sum_i R_i^{P*}=0 \quad (29)$$

$$-\frac{dP^{P*}}{dx}=\alpha\mu u^{P*}+\beta\frac{\rho_{gas}^*}{T^*}|u^{P*}|u^{P*} \quad (30)$$

$$x=0:\ \frac{1}{Pe}\frac{d}{dx}\left(\frac{p_i^{P*}}{P^{P*}}\right)=u_{x=0}^{P*}\frac{p_i^{P*}-p_{i,x=0^-}^{P*}}{P^{P*}}\quad\text{and}\quad u^{P*}=u^{P,in*} \quad (31)$$

$$x=1:\ \frac{d}{dx}\left(\frac{p_i^{P*}}{P^{P*}}\right)=0\quad\text{and}\quad P^{P*}=P^{P,out*} \quad (32)$$

$$N_i^*(x)=L_i^*\left[\left(p_i^{R*}(x)\right)^n-\left(p_i^{P*}(x)\right)^n\right] \quad (33)$$

where $\alpha=(150(1-\varepsilon)^2u_{ref}\ell)/\varepsilon^2d_p^2P_{ref}$, $\beta=(1.75(1-\varepsilon)M_{ref}u_{ref}^2\ell)/\varepsilon d_p\Re T_{ref}$, $R_i^{P*}=R_i^P/k_{\mathrm{PROX},ref}P_{ref}^{-0.08}$, $p_i^*=p_i/P_{ref}$, $P^*=P/P_{ref}$, $u^*=u/u_{ref}$, $R_i^{R*}=R_i^R/k_{SR,ref}C_{S1}^TC_{S1a}^TS_A$, $L_i^*=L_i/L_{ref}$, $x=z/\ell$, $Da=m_{cat}^R\Re T_{ref}k_{SR,ref}C_{S1}^TC_{S1a}^TS_A/\varepsilon u_{ref}A^RP_{ref}$, $R_A=A^R/A^P$, $R_{m_{cat}}=m_{cat}^P/m_{cat}^R$, $R_\kappa=k_{\mathrm{PROX},ref}/k_{SR,ref}C_{S1}^TC_{S1a}^TS_AP_{ref}^{0.08}$, $\Gamma=A^M\Re T_{ref}P_{ref}^{n-1}L_{ref}/\varepsilon u_{ref}A^R$, $Pe=\ell u_{ref}/D_{ax}$, M_{ref} is the reference molar mass, L_{ref} is the reference permeance coefficient of the membrane, x is the dimensionless axial coordinate of the reactor, Pe is the Peclet number for mass transfer, Da is the Damköhler number, Γ is the contact time (ratio between the permeate flow of reference component when fed pure for null permeate pressure and the total feed flow), $k_{SR,ref}$ is the rate constant for the steam reforming reaction at the reference temperature, $k_{\mathrm{PROX},ref}$ is the rate constant for the PROX reaction at the reference temperature, P_{ref} is the reference pressure (set to 100 kPa), T_{ref} is the reference temperature (set to 298 K), u_{ref} is the reference velocity and A^M is the permeation area of the membrane.

2.5. Numerical solution strategy

To simulate the steam reforming membrane reactor, it is necessary to solve equations (23)–(25) and (28)–(30) with the respective boundary conditions.

Table 1
Parameters for the simulation.

$Da \in [0.01–100]$	$\Gamma \in [0.5–4]$
$P^{R,out} = 400$ kPa	$P^{P,out} = 100$ kPa
T (K) $\in [473–493]$	S/C (H_2O/CH_3OH) $\in [1–3]$
$L_{ref} = 3.53\times10^{-7}$ kmol m^{-2} s^{-1} kPa^{-1}	$L^*_{H_2} = 1$
$L^*_{H_2O} = 0.313$	$L^*_{CH_3OH} = 0.001$
$L^*_{CO_2} = 0.08$	$L^*_{CO} = 0.015$

In order to overcome numerical instability problems, it was used the same strategy adopted already [29] for solving the equations: a time derivative term was added to their right-hand side, transforming this problem into a pseudo-transient one. The resultant partial differential equations were spatially discretized using the finite volumes method [30], being the partial pressure of component *i* determined with high-resolution schemes (WACEB) [31]. The advantage of using this high-resolution scheme is that it is bounded, which means that no unphysical oscillation occurs during the computed solution. The time advancement was accomplished by LSODA [32], a numerical package developed at the Lawrence Livermore National Laboratory. The solution was considered to be in steady state when the time derivative of each dependent variable and for each of the spatial coordinate was smaller than a pre-defined value.

3. Discussion

This study is focused on the advantages of adding a PROX catalyst into the permeate stream of a methanol steam reforming membrane reactor. The effect of several parameters in the enhancement of methanol conversion and hydrogen recovery is also studied. The developed mathematical model was previously validated by Sá et al. [33].

The operating parameters for the simulation are presented in Table 1. The steam to carbon ratio was varied from 1 to 3 according to what is commonly used in the literature [34]. The temperature was in the range of 473–493 K [35], the permeate pressure was set to 1 bar and the retentate pressure to 4 bar in order to achieve a high driving force. The sweep gas used was water vapour and the sweep ratio (ratio between the inlet permeate velocity and the inlet retentate velocity) was set to 1 [35]. After preliminary simulations, the concentration of oxygen in the permeate stream was set to 5% in order to achieve high carbon monoxide conversions. The hydrogen permeance was taken from Harale et al. [23]. The permeance data were used to estimate the contact time values, using feed flow rates and membrane areas commonly used in the literature [10,34]. The *Da* number range was estimated using the kinetic data from Peppley et al. [12] and the commonly used catalyst mass and feed flow rates [10,34].

3.1. Carbon monoxide permeation

As mentioned before, the CMS membranes present the drawback of being permeable to other species besides hydrogen. Among all compounds present in the reaction mixture, the removal of carbon monoxide is the most imperative once it poisons the anodic catalyst of the fuel cell. The permeation of carbon monoxide through the CMS membranes creates a permeate stream with concentrations above 10 ppm of this species, which must be reduced. As carbon monoxide is formed by the endothermic reactions methanol decomposition and reverse water gas shift (RWGS), their extent can be reduced by lowering the reaction temperature. In addition, the increase of the steam to carbon feed ratio can reduce the formation of carbon monoxide. The excess of steam will promote the SR reaction toward the products and less amount of methanol is decomposed to carbon monoxide. In the same way,

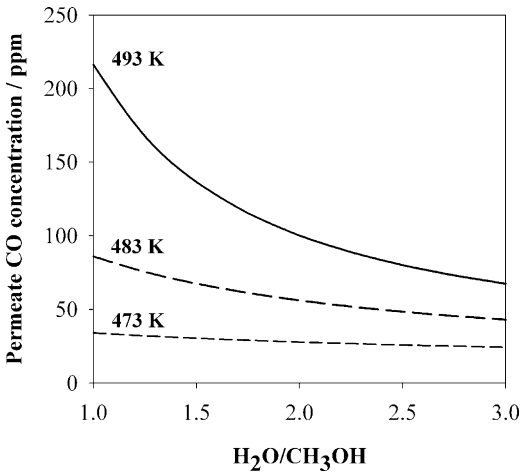

Fig. 2. Carbon monoxide concentration at the permeate side as a function of the temperature and the H_2O/CH_3OH feed ratio for a CMS membrane reactor. $Da = 50$ and $\Gamma = 2$.

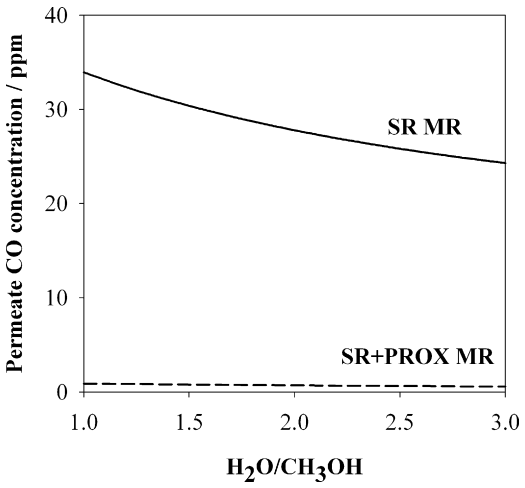

Fig. 3. Permeate CO concentration as a function of the steam to carbon (S/C) ratio for a SR MR and a SR + PROX MR. $Da = 50$, $\Gamma = 2$ and $T = 473$ K.

the WGS reaction is shifted toward the products, producing carbon dioxide and hydrogen and consuming carbon monoxide.

Fig. 2 illustrates these effects on the carbon monoxide concentration at the permeate side.

Although the amount of CO decreases with higher steam to carbon ratios and lower reaction temperatures, it still remains above 10 ppm and, thus, too high to be fed into a PEMFC. A strategy to reduce its concentration in the permeate stream is to promote its oxidation to CO_2, by adding a PROX reactor to the system. Some authors [36,37] placed a PROX reactor at the end of the SR reactor and reported good results in the decrease the content of CO. However, this implies a larger system with two reactors instead of one. Additionally, if all the CO produced in the SR reaction is converted to CO_2, a large amount of this species will be fed to the fuel cell, which has a negative effect on its performance [14]. In this thought of line, a different configuration is proposed, as shown in Fig. 1. By placing a PROX catalyst in the permeate side, the majority of CO that permeates through the membrane can be eliminated by reaction with O_2, producing CO_2. As the CO permeability through CMS membrane is low, only a small part of the CO produced in the retentate side permeates through the membrane, converting to CO_2 by the PROX reaction. This means that the performance of the fuel cell will not be compromised by the increase of the CO_2 concentration. In order to compare the purity of the permeate stream of a SR MR and a SR + PROX MR, Fig. 3 shows the permeate CO concentration for both systems.

As expected, the system SR + PROX MR shows clear advantages in what concerns the permeate CO concentration. The conversion of CO to CO_2 is very high, reducing the CO content to levels below 2 ppm. With this low concentration, is now possible to use the permeate stream to feed a PEMFC.

3.2. Carbon dioxide permeation

As mentioned before, in addition to the CO_2 that permeates through the CMS membrane, there is also a small amount that is formed in the PROX reaction at the permeate side. In order to minimize the negative effects of CO_2 on the performance of the fuel cell, its concentration should be maintained below 20% [14]. Accordingly, the contact time value, Γ, should be lowered as shown in Fig. 4. This parameter represents the ratio between a reference permeation flow and the feed flow. Accordingly, the higher the value of Γ, the higher is the fraction of the feed flow that permeates – the stage cut.

As can be seen in Fig. 4, lower values of Γ and Da result in lower CO_2 concentrations at the permeate side. As desired, the content of CO_2 is kept under 20% for all simulations. Nevertheless, lowering the contact time value can also present disadvantages by diminishing the amount of hydrogen that permeates. In the same way, small values of Da result in low methanol conversions. As so, it is essential to study which conditions enhance the performance of the membrane reactor.

3.3. Methanol conversion and hydrogen recovery

At high Damköhler numbers the reaction rates are high, which enhances the production of hydrogen as a consequence of increasing the methanol conversion:

$$X_{CH_3OH} = \frac{F^{R,in*}_{CH_3OH} - F^{R,out*}_{CH_3OH} - F^{P,out*}_{CH_3OH}}{F^{R,in*}_{CH_3OH}} \quad (34)$$

where F_i is the dimensionless flow rate: $F_i^* = p_i^* u^*/T^*$. Without doubt, the conversion should be as high as possible without the prejudice of a high purity permeate stream.

In order to find a compromise between high hydrogen production and high permeate purity, the influence of the Da number and the contact time in the methanol conversion is illustrated in Fig. 5.

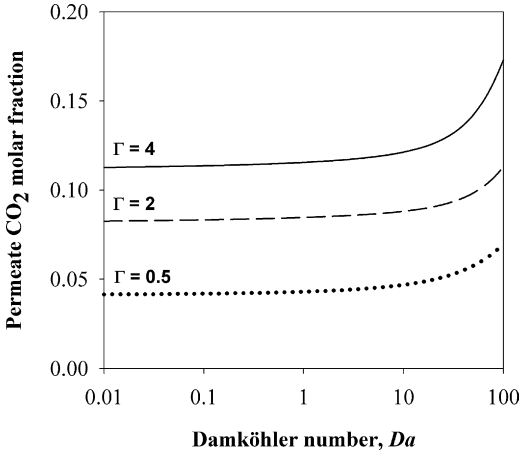

Fig. 4. Carbon dioxide molar fraction at the permeate side (dry basis) as a function of the Damköhler number for various contact time values. S/C = 3 and $T = 473$ K.

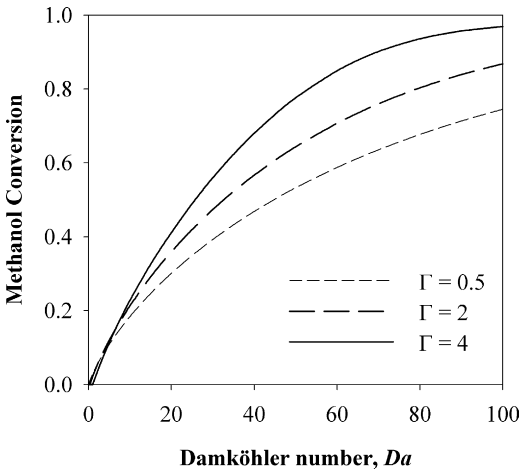

Fig. 5. Methanol conversion as a function of the Damköhler number for various contact time values. S/C = 3 and T = 473 K.

As expected, methanol conversion is enhanced by high *Da* numbers due to the high reaction rates. In addition, high contact time values represent high stage cut, thus high relative permeation flow. The increase of hydrogen permeation decreases its partial pressure at the retentate side and shifts the SR and the MD reactions toward the products, resulting in higher methanol conversion.

The hydrogen recovery is also an important factor to evaluate the performance of the membrane reactor. It represents the amount of hydrogen produced that is recovered at the permeate side – Eq. (35). The contact time and the *Da* number have a significant effect in this parameter as shown in Fig. 6.

$$\mathrm{Rec}_{H_2} = \frac{F_{H_2}^{P*}}{F_{H_2}^{P*} + F_{H_2}^{R*}} \tag{35}$$

Concerning the hydrogen recovery, the effect of the Damköhler number is different for high and low contact time values, as presented in Fig. 6. For this reason, the analysis must be made in two steps. First, at low Γ values, the membrane reactor operates at low stage cut. This means that the permeation flow is low compared to the retentate feed flow. At this stage, with the increase of the *Da* number, the amount of hydrogen produced increases and its partial pressure at the retentate side also increases. Consequently, the hydrogen driving force is higher, which should promote the increase of its recovery. However, Fig. 6 shows the opposite effect.

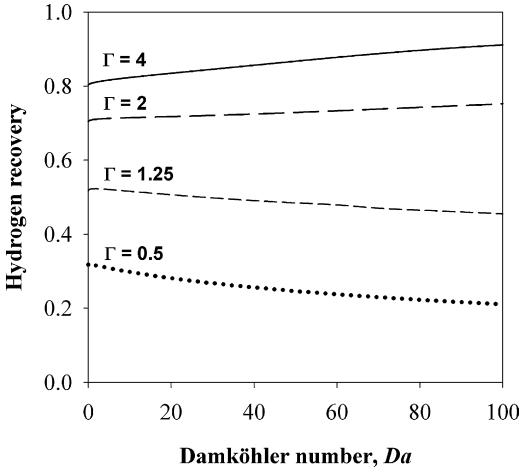

Fig. 6. Hydrogen recovery as a function of the Damköhler number for various contact time values. S/C = 3 and T = 473 K.

In fact, at low Γ values, the feed flow rate is high and the membrane area is small. As a result, only a minor part of the hydrogen produced is able to permeate through the membrane, being recovered at the permeate side. This means that the permeation does not compensate the increase of the hydrogen production, resulting in lower hydrogen recovery.

On the other hand, at high Γ values, the membrane reactor operates at high stage cut, and the relative permeation flow is also high. As explained before, the increase of the *Da* number results in higher hydrogen partial pressure at the retentate side, thus in higher driving force. As a result, most of the hydrogen produced permeates through the membrane, increasing the hydrogen recovery.

Compiling all the information gathered from Figs. 2 to 6, this system allows to achieve a hydrogen stream with CO concentrations below 2 ppm, CO_2 below 20%, high methanol conversion and high hydrogen recovery. If desired, the amount of CO_2 can be lowered to 10% by using a contact time value of 2 (Fig. 4), with a conversion of 85% (Fig. 5) and a hydrogen recovery of 75% (Fig. 6).

4. Conclusions

Two membrane reactors configurations were compared concerning the purity of the permeate stream, a common SR MR and a SR + PROX MR. It was shown that the presence of a PROX reactor at the permeate side positively affects the permeate stream composition. Unlike the SR MR, the SR + PROX MR converts almost all CO present in the permeate stream to CO_2. More specifically, the CO concentration at the permeate side was kept under 2 ppm and the CO_2 content remained below 20%. The main advantage of this MR configuration is the possibility of using the permeate stream to feed a PEMFC, without poisoning the anodic catalyst of the fuel cell.

It was also studied in which conditions the performance of the membrane reactor was enhanced in terms of methanol conversion and hydrogen recovery. In particular, it was concluded that methanol conversion is enhanced by the *Da* number and the contact time value, Γ. On the other hand, the hydrogen recovery increases with the *Da* number at high Γ, but decreases with the *Da* number at low Γ.

Finally, it was concluded that this system is appropriate to produce a hydrogen stream with CO concentrations below 2 ppm, CO_2 below 20%, high methanol conversion and high hydrogen recovery. If desired, the amount of CO_2 can be lowered to 10% by using a contact time value of 2, with a conversion of 85% and a hydrogen recovery of 75%.

Acknowledgments

The work of Sandra Sá was supported by FCT, grant SFRH/BD/30385/2006. The research was also supported by funds from FCT projects PTDC/EQU-EQU/71617/2006 and POCI/ENR/59323/2004.

References

[1] G. Cacciola, V. Antonucci, S. Freni, Technology up date and new strategies on fuel cells, J. Power Sources 100 (2001) 67–79.
[2] J.M. King, M.J. O'Day, Applying fuel cell experience to sustainable power products, J. Power Sources 86 (2000) 16–22.
[3] D. Ramirez, L.F. Beites, F. Blazquez, J.C. Ballesteros, Distributed generation system with PEM fuel cell for electrical power quality improvement, Int. J. Hydrogen Energy 33 (2008) 4433–4443.
[4] C. Stone, A.E. Morrison, From curiosity to "power to change the world", Solid State Ionics 152/153 (2002) 1–13.
[5] A.S. Damle, Hydrogen production by reforming of liquid hydrocarbons in a membrane reactor for portable power generation—model simulations, J. Power Sources 180 (2008) 516–529.
[6] D.G. Löffler, K. Taylor, D. Mason, A light hydrocarbon fuel processor producing high-purity hydrogen, J. Power Sources 117 (2003) 84–91.

[7] S. Ahmed, M. Krumpelt, Hydrogen from hydrocarbon fuels for fuel cells, Int. J. Hydrogen Energy 26 (2001) 291–301.
[8] J.C. Telotte, J. Kern, S. Palanki, Miniaturized methanol reformer for fuel cell powered mobile applications, Int. J. Chem. Reactor Eng. 6 (2008).
[9] A. Basile, A. Parmaliana, S. Tosti, A. Iulianelli, F. Gallucci, C. Espro, J. Spooren, Hydrogen production by methanol steam reforming carried out in membrane reactor on Cu/Zn/Mg-based catalyst, Catal. Today 137 (2008) 17–22.
[10] X. Zhang, H. Hu, Y. Zhu, S. Zhu, Methanol steam reforming to hydrogen in a carbon membrane reactor system, Ind. Eng. Chem. Res. 45 (2006) 7997–8001.
[11] B.A. Peppley, J.C. Amphlett, L.M. Kearns, R.F. Mann, Methanol steam reforming on $Cu/ZnO/Al_2O_3$. Part 1. The reaction network, Appl. Catal., A 179 (1999) 21–29.
[12] B.A. Peppley, J.C. Amphlett, L.M. Kearns, R.F. Mann, Methanol steam reforming on $Cu/ZnO/Al_2O_3$ catalysts. Part 2. A comprehensive kinetic model, Appl. Catal., A 179 (1999) 31–49.
[13] H.P. Dhar, L.G. Christner, A.K. Kush, Nature of CO adsorption during H_2 oxidation in relation to modeling for CO poisoning of a fuel cell anode, J. Electrochem. Soc. 134 (1987) 3021–3026.
[14] A. Bayrakçeken, L. Türker, I. Eroglu, Improvement of carbon dioxide tolerance of PEMFC electrocatalyst by using microwave irradiation technique, Int. J. Hydrogen Energy 33 (2008) 7527–7537.
[15] B.K.R. Nair, M.P. Harold, Hydrogen generation in a Pd membrane fuel processor: productivity effects during methanol steam reforming, Chem. Eng. Sci. 61 (2006) 6616–6636.
[16] C.-H. Fu, J.C.S. Wu, Mathematical simulation of hydrogen production via methanol steam reforming using double-jacketed membrane reactor, Int. J. Hydrogen Energy 32 (2007) 4830–4839.
[17] A. Iulianelli, T. Longo, A. Basile, Methanol steam reforming in a dense Pd–Ag membrane reactor: the pressure and WHSV effects on CO-free H_2 production, J. Membr. Sci. 323 (2008) 235–240.
[18] A. Basile, F. Gallucci, L. Paturzo, A dense Pd/Ag membrane reactor for methanol steam reforming: experimental study, Catal. Today 104 (2005) 244–250.
[19] M.P. Harold, B. Nair, G. Kolios, Hydrogen generation in a Pd membrane fuel processor: assessment of methanol-based reaction systems, Chem. Eng. Sci. 58 (2003) 2551–2571.
[20] M.D. Falco, Pd-based membrane steam reformers: a simulation study of reactor performance, Int. J. Hydrogen Energy 33 (2008) 3036–3040.
[21] G.A. Sznejer, I. Efremenko, M. Sheintuch, Carbon membranes for high temperature gas separations: experiment and theory, AIChE J. 50 (2004).
[22] A.F. Ismail, L.I.B. David, A review on the latest development of carbon membranes for gas separation, J. Membr. Sci. 193 (2001) 1–18.
[23] A. Harale, H.T. Hwang, P.K.T. Liu, M. Sahimi, T.T. Tsotsis, Experimental studies of a hybrid adsorbent-membrane reactor (HAMR) system for hydrogen production, Chem. Eng. Sci. 62 (2007) 4126–4137.
[24] D.L. Trimm, Minimisation of carbon monoxide in a hydrogen stream for fuel cell application, Appl. Catal., A 296 (2005) 1–11.
[25] Y. Choi, H.G. Stenger, Kinetics, simulation and insights for CO selective oxidation in fuel cell applications, J. Power Sources 129 (2004) 246–254.
[26] S. Ergun, Fluid flow through packed columns, Chem. Eng. Prog. 48 (1952) 89–94.
[27] P.V. Danckwerts, Continuous flows systems – distribution of residence times, Chem. Eng. Sci. 2 (1953) 1.
[28] H.C. Lee, D.H. Kim, Kinetics of CO and H_2 oxidation over $CuO–CeO_2$ catalyst in H_2 mixtures with CO_2 and H_2O, Catal. Today 132 (2008) 109–116.
[29] J.M. Sousa, A. Mendes, Simulation study of a dense polymeric catalytic membrane reactor with plug–flow pattern, Chem. Eng. J. 95 (2003) 67–81.
[30] P. Cruz, J.C. Santos, F.D. Magalhães, A. Mendes, Simulation of separation processes using finite volume method, Comput. Chem. Eng. 30 (2005) 83–98.
[31] B. Song, G.R. Liu, K.Y. Lam, R.S. Amano, On a higher-order bounded discretization scheme, Int. J. Numer. Methods Fluids 32 (2000) 881–897.
[32] L. Petzold, Automatic selection of methods for solving stiff and nonstiff systems of ordinary differential equations, Siam J. Sci. Stat. Comput. 4 (1983) 136–148.
[33] S. Sá, H. Silva, J.M. Sousa, A. Mendes, Hydrogen production by methanol steam reforming in a membrane reactor: palladium vs carbon molecular sieve membranes, J. Membr. Sci. 339 (2009) 160–170.
[34] F. Gallucci, A. Basile, Co-current and counter-current modes for methanol steam reforming membrane reactor, Int. J. Hydrogen Energy 31 (2006) 2243–2249.
[35] F. Gallucci, A. Basile, Pd–Ag membrane reactor for steam reforming reactions: a comparison between different fuels, Int. J. Hydrogen Energy 33 (2008) 1671–1687.
[36] Y. Men, G. Kolb, R. Zapf, D. Tiemann, M. Wichert, V. Hessel, H. Löwe, A complete miniaturized microstructured methanol fuel processor/fuel cell system for low power applications, Int. J. Hydrogen Energy 33 (2008) 1374–1382.
[37] T. Kim, S. Kwon, MEMS fuel cell system integrated with a methanol reformer for a portable power source, Sens. Actuators A: Phys. 154 (2009) 204–211.